

Chapter 6

A New Perspective on Growth of GaN from the Basic Ammonothermal Regime



Elke Meissner, Dietmar Jockel, Martina Koch, and Rainer Niewa

Abstract Although the crystal growth of GaN under ammonothermal conditions is being performed for quite some years now, the physical processes going on in the autoclave are still debated. Insight in the autoclave by in situ techniques is difficult and numerical simulations are based on physical models where the experimental prove is eventually vague. This chapter reports a period of experimental work leading to a new vision of the basic ammonothermal process. We shortly summarize the 3D thermal- and transport model and a first chemical model. Subsequently, we propose an alternative picture for the ammonobasic crystal growth of GaN, which not only leads to consequences with regard to required pressures and temperatures but also to a potential new growth process. The proposed hypothesis and empirical model involves the presence of a liquid phase in the autoclave in form of an amidogallate complex.

6.1 Introduction

Nowadays the importance of semiconductor crystal growth is still unbroken. The growth of large crystal bodies enables the production of semiconductor wafers for the fabrication of electronic devices. However, the semiconductor materials are very different with regard to the crystal growth techniques which could be applied for the growth of volume crystals. Amongst the new compound semiconductors with wide

E. Meissner (✉) · D. Jockel · M. Koch

Chair for Electron Devices, University of Erlangen-Nuremberg, Cauerstr. 6,
91058 Erlangen, Germany

e-mail: elke.meissner@iisb.fraunhofer.de

E. Meissner

Fraunhofer Institute for Integrated Systems and Device Technology, Schottkystr. 10,
91058 Erlangen, Germany

R. Niewa

Institute of Inorganic Chemistry, University of Stuttgart, Pfaffenwaldring 55,
70569 Stuttgart, Germany

© Springer Nature Switzerland AG 2021

E. Meissner and R. Niewa (eds.), *Ammonothermal Synthesis and Crystal Growth of Nitrides*, Springer Series in Materials Science 304,

https://doi.org/10.1007/978-3-030-56305-9_6

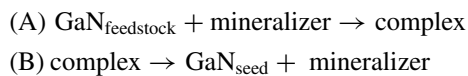
band gaps and in front of the developing markets, it is not much disproportionate to say, the GaN is the second most important semiconductor after silicon [1, 2].

In ammonothermal crystal growth, evidently the problem is, that many essential observations which would be needed to explain the ongoing processes cannot be made in situ due to the pressurized growth system. So the understanding of transport processes inside the autoclave is very limited and explanations often vague. In this chapter we describe a different view on the existing understanding of an ammonobasic growth regime, based on our own experimental observations during the last years. Even though some of the conclusions may have speculative aspects, there is enough experimental evidence for a new vision.

The ammonothermal crystal growth is usually considered a solution growth process. The GaN shall be solved in the supercritical ammonia at a given thermodynamic pair of temperature and pressure. However, a solution growth process and the resulting growth rates depend on the amount of material that can be dissolved in the solvent. The solubility of GaN in pure supercritical ammonia is not very high, respectively nearly zero. Therefore, the so called mineralizers are added to the system, which should help to solve enough GaN through the formation of an intermediate species. The intermediate can be transported to the place of crystallization at the location of the seeds where the GaN crystalizes. So the action of the mineralizers is at least twofold. Many different mineralizers were used in the past years which all act differently depending on the chemical environment they create. Also the habit and even the structure of the GaN crystals can change from hexagonal to cubic in relation to the mineralizer as described in e.g. [3, 4] and references therein. In this chapter we concentrate on the basic ammonothermal regime. However, some consideration will also be valid for acidic ammonothermal processes.

Not much is known about the nature of the intermediates. The newest findings are described in Chap. 13. The mineralizers in the ammonobasic system shall form a complex which must be transported from the source (the place of dissolution of the GaN feedstock) to the seeds (place of crystallization) in the autoclave. In the ammonobasic regime the complex is likely a tetraamidogallate ion. Solid alkali metal compounds comprising this complex ion were described by some authors [5–7]. However, a full description of the growth process of GaN inside the autoclave, including the chemical reactions, is very difficult due to the limited options for direct observation.

In a former study by the first author's group, published by Erlekampf et al. [8] and Seebeck et al. [9] we reported the study of the temperature fields and related convection patterns, established in the autoclave, in order to facilitate the transportation of the complex through the system and suggested a first transportation model based on the formulation of two basic transport channels. The model is simply assuming the following two general processes (A) and (B):



In the process (A) the GaN feedstock will be dissolved by the aid of the mineralizer and the Ga-containing complex is formed, which transports Ga to the seed crystals. There the crystal growth can happen by the process (B), which is the formation of GaN from the complex in the presence of the ammonia. In turn, the mineralizer is released from the complex and reformed. Through that “backward channel” the mineralizer must be transported back to the feedstock region in order to start the process of dissolution again, which means that, a constant transportation action is required in order to continuously drive the system forward. From the first, this description is independent on the type of growth environment and the applied orientation of the temperature field. However, the directions of mass and heat transport will depend on the choice of the mineralizers. The basic idea is to always have the hotter zone at the bottom of the autoclave in order to profit from convection, due to natural buoyancy, no matter what the chemical processes inside the autoclave are. For the ammonobasic regime this results in a geometry where the seeds are placed at the bottom of the autoclave and the feedstock at the top, which is also described in the literature from groups working in the ammonobasic regime e.g. [10–13]. As this configuration emerges from the fact that a retrograde solubility for GaN was described for the usage of typical ammonobasic mineralizers, like the alkali metal amides LiNH_2 , NaNH_2 or KNH_2 creating the NH_2^- ions in the solution, one of the biggest benefits could be, that unwanted impurities in the grown crystals may have an opposite transport direction in case of an own regular solubility. Thus, such impurities would be less incorporated into the crystals, as crystallization under retrograde solubility will not happen at the place of low temperature like in classically crystal growth, but instead at the higher temperature zone of the growth setup. So the impurities should be transported away from the surface of the growing crystal. On the other hand the transport direction of the “backward channel” (B), where the mineralizer releases from the complex after formation of the GaN and should be transported back to the feedstock region at the top of the autoclave for solving new material, would be opposite gravity. This functions trough the up-flow, induced by the implementation of the thermal field and relative positions of feedstock and seed as described before. On the other hand the complex must be transported “downwards” with the gravitation vector but against natural buoyancy. So how the transport of chemical species is really established may be quite complex in the ammonobasic crystal growth of GaN as also solubilities of many mineralizers are thought to be retrograde. In turn this means that a compound with a retrograde solubility can be probably transported back to the zone of dissolution, but solubility would decrease at the same time.

The first considerations that we made for a chemical model, based on the numerical simulations performed by Erlekampf et al. [8] and Seebeck et al. [9], will be discussed later in this chapter. The chemical model we propose is however preliminary and describes fundamental principles based on existing observations, but would of cause benefit from more data and further studies of crystal growth rates for different configurations and places in the autoclave related to the temperature, convection, concentration fields, type of mineralizers and pressure conditions during the growth process. Wang et al. [14] published an empirical vision about mass transport and

the ongoing processes in the autoclave but did not perform numerical simulation or attempt to further quantify.

The knowledge of the nature of the dissolved complex is very important, not only for the inclusion of the chemical species in the numerical model, but also for the considerations with regard to the growth kinetic of the crystals. Additionally, not only the growth rates of crystals would be interesting, but also the observation of growth instabilities, growth habits or facet morphology which contains information about the growth kinetic or rate limiting steps. A small number of papers describe the growth habit of the crystals e.g. for the different mineralizers used in the growth process [14–20]. The growth rates and shapes of the crystals, are of course important and contain information about the growth process. From classical theory of solution growth the presence of solvents can change the shape of the grown crystals. The fundamentals of the related PCB (Periodic Bond Chain) theory can be found at Hartmann and Perdock [21] or its revisits [22, 23]. Many observations stem from the solution growth of KH_2PO_4 (KDP) crystals e.g. [24–26] or other e.g. [27] and references therein, which could be easily observed in situ during the growth process in the applied environment. The knowledge about the nature of all transported species in the basic ammonothermal process and the involved intermediate complex would be essential for the description of surface energies budgets. On the other hand there are many impurities underway in an ammonothermal autoclave, due to the corrosive action of the supercritical ammonia together with the mineralizers at high pressure and temperature. These impurities may additionally change the expected equilibrium shape or growth rates of the crystal if they are collected on a growing surface, modify the boundary layer or local supersaturation, which may also result in growth instability. This cannot be taken into account easily in theoretical considerations. So, in this sense the final shape of the crystal grown from an ammonothermal process is hardly predictable and difficult to judge and it is likely not possible to distinguish between the individual contributions.

Growth rates documented in literature are manifold resulting from different ammonobasic and acidic processes using various mineralizers, liner materials and different impurity contents in the process. Usually, growth rates between 20 and 100 μm per day were achieved for the basic ammonothermal process [28]. The special growth technique for ammonoacid growth, developed by Ehrentraut et al., resulted in about 5–100 times higher growth rates than conventionally observed [29], which may be obvious from the higher solution temperatures and pressures possible in their system. Due to the ammonoacid condition the dissolution takes place at higher temperatures and crystallization happens at lower temperatures. Ehrentraut et al. reported about 30–40 $\mu\text{m}/\text{h}$ growth rate which could be routinely established and is the highest growth velocity reported so far. Interestingly the authors find this possible for all crystallographic directions. So basically for ammonoacidic technique an establishment of a stronger driving force for crystallization is present, obviously due to higher possible supersaturation. The observation of growth rates in general can be taken as a measure for the limitations of the growth process and growth kinetics involved.

Usually the growing crystal in an ammonothermal reactor cannot be directly observed. Special analytical setups are necessary for operando observations in the autoclave, like described and elaborated in other chapters of this book. Beside the in situ measurements, the only way to better understand and describe the growth process is the observation of shape and growth rates of crystals in relation to the position in the autoclave for a given growth process and the correlation of such data with a model understanding of heat and mass transport. Ideally combined with a chemical model, involving the transportation of the chemical species in the flow fields, this could give a full picture about the ongoing processes and how to control them.

This chapter on the one hand reports the results of a research project spanning from in situ temperature measurements, development of a 2D and 3D model describing temperature fields and convection transport as well as the development of a first chemical model, which can be further advanced and adjusted to different process conditions of ammonothermal growth processes. On the other hand the focus of this chapter will be the description of an alternative picture of the basic ammonothermal growth process. This view results from the observations made during the course of the project and involves a liquid phase of intermediates in the autoclave, which was not considered before as present compound during the growth run. This may promote and advance further discussion and understanding of the results from crystal growth in supercritical ammonia in general and offers new options for the design of a growth process for GaN.

6.2 Experimental Details

The experiments described in this chapter were performed in autoclaves suitable for ammonobasic conditions and made out of Inconel alloy 718. Due to the processing in the ammonobasic regime the inner wall of the autoclave was not coated with a liner, since corrosion is minimized in ammonobasic milieu. A detailed study on the corrosion of autoclave material can be found in Chap. 11 of this book. The autoclave has a range of safe usage from room pressure up to 300 MPa and a temperature range up to 600 °C under pressure. The experimental conditions of the experiments performed during this study made use of the full span of possible conditions. The inner setup differed slightly as a result of the design of individual experiments e.g. with regard to the relative positioning of feedstock and seeds. The inner setup was also fabricated out of Inconel parts. Two versions of an autoclave with upper and lower flange or with only a top flange were used. Additionally, a flange with five feed troughs for thermocouples (TCs) was available for the in situ temperature measurements that were performed in order to validate the numerically calculated 2D temperature distribution in the autoclave. This “temperature-measurement-flange” could be used with the double flange autoclave. As the filling and pressurization could be still realized from the top in that case, the TC-flange would be placed as bottom flange. For the experiments either of the autoclaves was placed in a three zone or two zone

furnace, which also offered the possibility of an air gap or local cooling in the middle of the setup for the eventual creation of a thermal knife or implementation of local steep temperature gradient. The components were chosen to offer maximum flexibility for the complete setup. The heater cassettes can be opened as half shells such that the autoclave can be placed inside together with a fitting insulation for the best possible stability and most accurate control of the temperature fields around the autoclave body. Figure 6.1 shows as an example the autoclave with the upper and lower flange in front of the two zone furnace for illustration of the setup and at the right hand side the temperature measurement flange with mounted thermocouples, type K with Inconel mantle.

The filling with ammonia was performed by condensation of the cold ammonia into the autoclave. The filling degree is calculated for $T = -33\text{ }^{\circ}\text{C}$, the amount of ammonia condensated into the autoclave was measured by weighting and at a later point by direct monitoring of the filling height by ultrasound measurements through the outer wall of the autoclave. This type of determination of degree of filling is considered precise and is described detailed by Baser and Schwieger in Chap. 7 of this book. The autoclave was loaded with the feedstock, seeds and mineralizers under inert gas condition inside a glove box and afterwards attached to the high pressure system for pump and purge cycles with N_2 and subsequent ammonia filling. As seeds and feedstock material we used trimmed GaN crystal pieces made by hydride vapor phase epitaxy (HVPE) and broken pieces of bulk GaN crystals. The mineralizer was

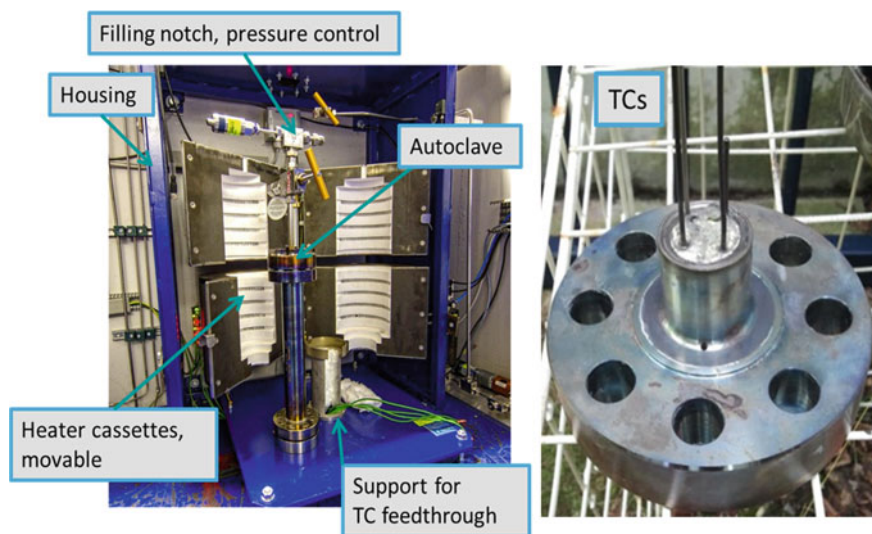


Fig. 6.1 Left picture: image of the opened 2-zone furnace setup. The autoclave with the two flanges is placed on the support-foot in the center during the experiments. The picture shows the support foot for the temperature measurement flange which would be the bottom flange. Right picture: image of the temperature measurement flange with the thermocouples (TCs) reaching to the inside volume of the autoclave after mounting

weighted and brought into the autoclave in form of a powder compacted inside a small net-cup. At a later point in the study, the mineralizer was placed underneath the seeds, for the purpose that will be described later in the chapter. As mineralizer we used KNH_2 , NaNH_2 or KN_3 in different concentrations. As this refers to an ammonobasic regime, a retrograde solubility is expected. More details will be mentioned at the individual experiments described in the results section since the setup for some experiments changed after the target of the runs. All materials loaded into the autoclave were weighted. At the end of the processes the autoclave was cooled down and depressurized. After opening, the interior was washed with water and alcohol in order to dissolve the residual mineralizer and capture the grown crystals and residual feedstock for determination of weight, size and mass balance. The total mass balance will not be further used later on, as the value is quite inaccurate due to deposition not only on the seeds but also elsewhere in the autoclave. In case any liquid phase separated from the water/alcohol mixture (which we used for solving the residuals in the autoclave after opening), it was collected as well, as will be described later in the chapter. The source material as well as the crystalline material which was deposited was investigated by different microscopic means. The layer thickness of the newly grown GaN was measured by microscopy from the cross section of the seeds. This values were also used to determine the growth rates. The geometry and weight change were used to determine the amount of etching and deposited material. The shaped seeds (regular and kinetic seeds) were investigated by microscopy with respect to the crystal faces that developed.

For the description of the temperature field and the development of a 3D model of the thermal and convective fields in the autoclave, as well as the development of a first chemical model of an ammonothermal process, we used combinations of numerical 2D simulations and 3D simulations in order to reveal non axisymmetric effects. The details for the numerical simulations can be read elsewhere [8, 9]. The numerical description of the thermal field and flow pattern were not only utilized for the understanding of the mass and heat transport but also for the design of the inner components like the baffle plate and their action with regard to transportation of the intermediate species from the feedstock to the seed region. Calculations were done for an autoclave aspect ratio of 1:20, which is very common.

6.3 Results and Discussion

6.3.1 Calculation and Validation of the Temperature Fields

First we studied the temperature distribution in the autoclave as this is essential for the crystal growth and the design of the furnace-heater-system and insulation. The temperature fields were calculated by numerical simulation and directly measured using a special flange with through feeds for 3–5 thermocouples, resistive enough to the corrosive environment. The results of the direct temperature measurements

validated the numerical calculations and confirmed first of all the correctness of the 2D temperature distribution model. The details were earlier reported [8, 30]. The calculated 2D temperature field was taken as a boundary condition for the 3D model to calculate the convection pattern and mass transport. For the calculation of the transport of species the respective molar weights of involved species were taken to calculate solutal buoyancy. As species involved in the process we considered the GaN, a gallium carrying complex as intermediate and the mineralizer. The results of the calculations were described in detail in our former publications [8, 9]. The findings showed e.g. that the geometry of the inner autoclave parts is essential for the steering of the mass flow which is kind of intuitive. However, it also turned out that the convection pattern is neither independent on time nor axis symmetric and cannot be described accurate enough with a 2D axis symmetric calculation only, which does represent the vast majority of the published data [31–34]. In [9] we showed the action of the shaping and positioning of the baffle plate, placed e.g. in the center of the autoclave, which can result in a drastic enhancement of mass transport along the axis of the autoclave. Such action is particularly important in the case of the ammonobasic regime where the transport can be expected to be low because it is contrary to natural convention. It could be also shown by the 3D approach that there are significant fluctuations of the temperature and flow velocity which are highest close the baffle plate. The dissolution of the feedstock may be mainly governed by diffusion, so strong fluctuations at the dissolution zone around the GaN source block are clearly favorable as the mixing and steering of the solution would be enhanced. On the other hand, inside the crystallization zone, where the crystals should have a most controlled environment with stable temperature field and transport rates, such fluctuations would be unfortunate and could dramatically deteriorate the quality of the growing crystals. This would be especially critical for bigger scale autoclaves in an industrial environment, when many seed crystals are placed inside an autoclave at the same time.

For transport of the species we additionally considered the contribution of solutal buoyancy. Which is not the case in the existing publications on numerical simulation of ammonothermal process. The results of our calculations were reported in [8, 9]. With the chemical model we formulated it was possible to calculate local time averaged concentration profile of the involved chemical species, which showed that the mineralizer can collect at places in the autoclave under certain circumstances and by that could not contribute to the growth process any more. We moreover found that the solutal buoyancy makes a significant contribution to mass transport, in quantity comparable to thermal induced transport. It could be concluded that the transport of species cannot be described good enough only based on the convection patterns. The work demonstrated the importance of a suitable transportation model for the chemical species involved in the growth process. The first chemical model we suggested, could—in further developed state of cause—allow to calculate true concentration patterns for a chosen setup and geometry of inner autoclave parts like e.g. baffle plates. This would be particularly important for larger industrial scale autoclaves. However, in any case all the numerical models were calculated for the case of a full supercritical system. No other phases than the solid and later dissolved

GaN, the crystallized GaN in solid form and the mineralizer with the intermediates dissolved in the supercritical ammonia were taken into account so far.

6.3.2 *Crystal Growth Experiments*

In all processes performed it was generally difficult to run the experiments for a long time as the tightness of the sealings evolved more and more critical with the total duration of a run. This was also due to the fact the experiments were often performed at the technical specification limits of the components and quite a number of runs failed to run until the end. However, some of the growth runs experienced a spontaneous pressure drop due to the breakage of the rupture disc. Experiments with unexpected spontaneous pressure drop were of course unfortunate as not running to plan, but turned out to be very informative. In all of such respective processes the growth rates of the material crystallized on the seeds was found to greatly exceed the growth rates of the experiments which run to the end as planned at constant pressure. This was from the first glance unexpected and counterintuitive, also with regard to the numerical calculations and the transport possibilities as well as to the existing literature. The later experiments were such designed that the explanation of those observations could be formulated, which lead to a different understanding of the basic ammonothermal process for the deposition of GaN, compared to the existing literature. This chapter reports the interpretation of the results achieved during the study and as a result a corresponding model of growth of GaN from an ammonobasic process involving a liquid phase. To our knowledge there is no publication describing the ammonothermal crystal growth of GaN including the action and the formation of a liquid intermediate. The formation of liquid compounds with ammonobasic mineralizers KNH_2 , RbNH_2 and CsNH_2 was described by some authors Zhang et al. [35], Molinie et al. [36], Wang and Callahan et al. [37]. Whether such compound eventually exists in its liquid form under the experimental conditions of the ammonothermal growth experiments was so far unknown.

Figure 6.2 shows on the left side the principle setup of the experiments and on the right hand side a graph of experiments performed. The resulting materials crystallization is indicated first of all simply as happened (deposit, red symbols in the figure) or not happened (no deposit, black symbols in the figure). In the experiments, qualitatively spoken, a deposition of GaN was measured or not at the place of the seeds at the bottom of the autoclave. Deposition or not was identified as a positive or negative weight change or by a visual and microscopic inspection. The plotted temperature data refers to the temperature at the bottom of the autoclave as measured by thermocouples at that place. The pressure is given as the maximum pressure that was achieved or maintained during an experiment. Three experiments are special marked with a blue rim. The three marked red squares with the blue rim represent growth runs that had a remarkable deposition, although the experiment experienced a sudden drastic pressure drop during the run time and then proceeded regular for the rest of the process time at a lower pressure. We would have expected that those

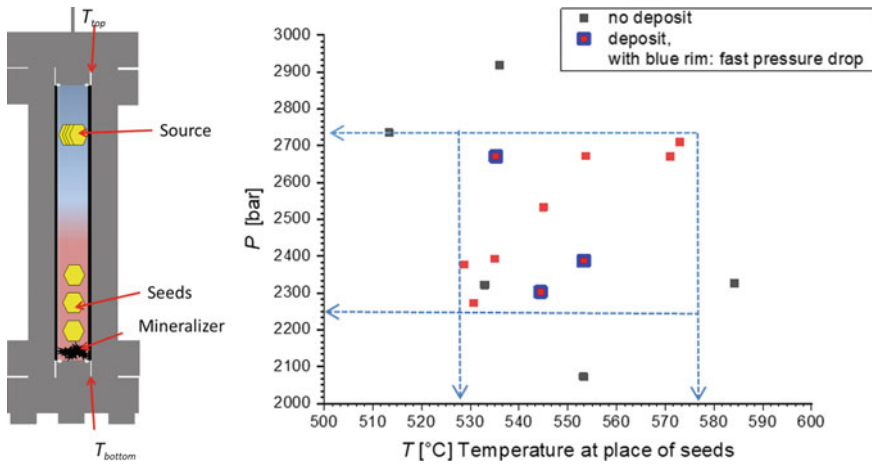


Fig. 6.2 Schematic drawing of the experimental setup (left) and experimental results in terms of positive (red symbols) or no deposition (black symbols) of GaN on the seeds. Three experiments are marked where deposition took place although the experiment experienced a fast pressure drop (red symbols with blue rim). Dashed lines represent the boundary conditions where growth on the seed was possible

experiments would lead to no deposition, which was not the case. On the other hand, these experiments turned out to be important for the total interpretation of results.

Of course in this diagram, we ignore for the moment the solubility, the quantitative amount of mineralizer (KNH_2 in this cases) other than simply the fact “enough mineralizer”, and an existing temperature gradient between the source zone and the place of crystal growth. However, involving these parameters may result in the same factum, whereby the influence of the pressure as a parameter in the crystallization of GaN on a seed is so far unclear. From that diagram, a GaN deposition could be achieved for the following boundary criteria:

$$\sim 2250 \text{ bar} < p \sim 2730 \text{ bar}$$

and

$$\sim 530 \text{ }^\circ\text{C} < T \sim 575 \text{ }^\circ\text{C}$$

The interesting results appear, if the data is analyzed for any individual experiment and simple fundamental assumptions. From this point of view, a crystallization can only happen if a supersaturation exists such that the system is slightly pushed out of equilibrium and simply more deposition than dissolution happens. So, a most simple postulate would be that at those experiments where a deposition of GaN was found, a high enough supersaturation was achieved on the surface of the seeds. From theoretical consideration one would expect that the dissolution of the GaN from the feedstock and the transport of the Ga-containing complex to the place of crystallization should be first of all a function of temperature and transportation in the

autoclave. For the ammonobasic case one would expect that the dissolution of GaN and formation of transported intermediate is higher at lower temperatures as a result from the retrograde solubility with potassium amide mineralizer. Supersaturation could occur if enough GaN was dissolved at the source zone and mass transport in the autoclave towards the seed region was high enough. These conditions were obviously fulfilled for the boundary criteria given above.

After the first chemical model we proposed, a supersaturation can be created if the complex was formed at the source zone and the transported intermediate species in the autoclave has a high enough concentration at the growth zone. Then, if the GaN crystallizes the mineralizer will be released, transported back and dissolves again the source material. So, as a consequence the area in Fig. 6.2 where the GaN could be crystallized, can be considered as kind of a stability field of the existing intermediate phase for the respective experimental conditions. Without the intermediate phase above a critical concentration no crystallization would happen. The only black point falling into that field represents an experiment that was accidentally stopped, shortly after the autoclave reached the experimental conditions. As a result there was either not enough time for the formation or the transportation of the complex and in consequence the concentration of the intermediate at the surface of the seed was not high enough, to create a supersaturation and finally no deposition of GaN took place. Otherwise, for a longer run time (as originally anticipated) the formation of GaN on the seed would have to be expected. Thus, we consider that particular experiment as belonging to the set of “red” points.

One can conclude that the intermediate phase would not exist much above a threshold pressure of roughly 2730 bar and not below 2250 bar, respectively, not much below a temperature of approximately 530 °C and no more above 575 °C; or at least not in the form that was effective for the crystallization of the GaN with KNH_2 mineralizer in the given set of experiments. Figure 6.3 shows the collected data together with a line through the red data points at or below which the crystallization of GaN should be expected. The line is meant as eye guide and does so far not represent a fit of a physical model to the data points. However, it indicates a nonlinear relation between the pressure and temperature condition for the formation of the complex.

There is some scatter of the experimental data laying close around that line. Due to the complexity of the experimental situation, we did not calculate numerical error bars, but visualize the uncertainty region by the gray shaded area. As below that line, GaN crystallization can be expected until the lower threshold values are reached, we consider it as the boundary curve for the stability field of the intermediate complex. Of course, a much larger number of experiments would be necessary, in order to truly verify an equilibrium curve for the stability field of the particular intermediate involved in the case of the applied KNH_2 mineralizer.

Now, the experiments with the blue-rimmed red symbols will be discussed (#1–#3 in Fig. 6.3). As in that growth runs the deposition of GaN on the seeds was observed, we count them to lay inside the existence field of the intermediate, at some point in time during the course of growth run, although, they came to lay outside the grey shaded area, with respect to the experimental conditions. Obviously, it happened

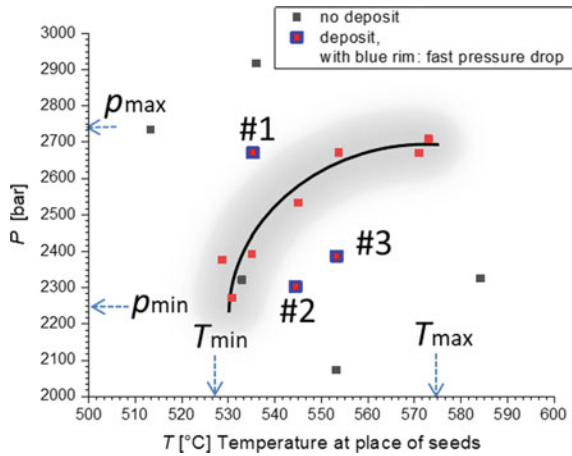


Fig. 6.3 Estimated boundary line for the stability region of the intermediate complex involved in the experiments. Below T_{\min} and P_{\min} and above T_{\max} and P_{\max} a deposition of GaN is not expected. The line is an eye guide and does not represent a physical model. The gray area visualizes the scatter interval

to have enough supersaturation around the seed to create a GaN deposition, especially for #1 which was initially far above the boundary curve, close to T_{\max} . These experiments are marked and have to be discussed differently as they experienced a sudden pressure drop shortly after the start of the run time. However, a remarkable deposition of a thick layer of GaN was found on the surface of the seeds. The growth of that material could not be the same “regular” growth as in the experiments marked with the red squares in Figs. 6.2 and 6.3. It could as well not have occurred due to supersaturation based on the temperature and transport gradient established between the source and the growth zone, nor could it have occurred directly from the supercritical phase, as this was released from the autoclave due to the pressure drop after sudden leakage. A fast growth directly from the supercritical phase as a result of a solubility limit excess would have resulted likely in a kind of mass crystallization of many polycrystals, which was not observed. Instead the GaN deposit occurred in form of a thick epitaxial layer on the seeds. The growth happening in this experiment can be understood, if the pressure drop would cause the intermediate complex to dissociate, fall under the stability limit in terms of pressure and release the gallium. This means in a consequence, that the complex transporting the Ga may dissociate with temperature rise, but is stabilized by the pressure. In this case the temperature was nearly constant and dropped only minor (measured by the bottom thermocouple) and could not likely cause the dissociation of the complex. Instead, because the pressure was decreasing rapidly due to the unplanned pressure loss, the complex could decompose, which caused the growth of a crystalline GaN layer. If a lower total pressure or a huge pressure gradient would be taken into account the respective data point may fall into the grey area. The #2 and #3 experiments are below the boundary curve but inside the temperature window where we usually observe a

GaN growth on the seeds. Although they experienced an accidental pressure loss, which would cause additional dissociation of the complex, the GaN deposition was expected. So the pressure drop brought them out of the planned p , T condition and the stability field of the complex, but the fast pressure drop decomposed the complex additionally and growth rate was higher than usual. Both of the points #2 and #3 would rather move to lower temperatures if the pressure release would cause a slight temperature drop and by that may fall as well into the grey zone or get closer to it.

As a conclusion it can be stated, that the growth of GaN in the ammonobasic regime with KNH_2 mineralizer occurs if the system is hold between p_{\max} and p_{\min} and T_{\max} and T_{\min} . According to the chemical model, suggested before, the transported complex must be dissociated in order to release the Ga for the formation of GaN. This can be achieved by either $p = \text{const.}$ and $T \neq \text{const.}$ within the given p and T boundaries (red points in the diagram) or for $p \neq \text{const.}$ and $T = \text{const.}$ (the pressure drop experiment). This implies that the intermediate compound in the potassium containing ammonobasic regime is stable within that p and T boundaries. The corresponding intermediate is thought to be a tetraamidogallate ion or condensation products thereof [38]. As below $p_{\min} \cong 2250$ bar and $T_{\min} \cong 530$ °C no growth occurred, the complex could obviously not be formed, whereas above $p_{\max} \cong 2730$ bar it may no more exist. Alternatively, the complex exists but is stabilized by the pressure and cannot be dissociated enough to release the gallium. The temperatures beyond $T_{\max} \cong 575$ °C may lead to a thermal decomposition of the complex irrespective of the pressure, as the curve sketched above implies a “flattening” rather than a continuous rise, which would be in accordance to fundamental thermodynamics as the Gibbs free energy depends on T and p differently.

The following diagrams show how much of the GaN source material was dissolved as a function of temperature or pressure for the application of KNH_2 as a mineralizer. From this plots there is no clear correlation with either of the parameters p or T . However, it looks more like a peak function, which was put to the graph for illustration; it does not represent the fit of a physical model. If it can be assumed that the formation of the gallate is a prerequisite for the mass dissolution of GaN at the source zone, this should more or less correspond to the stability field of the complex as describe before. The difference to the curves discussed above is that Fig. 6.4 shows the situation at the source zone, whereas Figs. 6.2 and 6.3 are monitoring the situation at the seed position. In terms of pressure dependence the threshold of slightly above 2000 bar is also visible which corresponds to the described stability field of the complex discussed above. With view to temperature the picture is a little different as the lowest temperature at the crystallization zone where growth on the seed was observed was approximately 530 °C and with higher temperature the growth increased, which indicates a retrograde temperature behavior of solubility of the Ga carrying species in the supercritical NH_3 between 530 °C and T_{\max} . This is not unexpected as described before in the literature. The mass dissolution of GaN measured at the source zone is highest around 400 °C.

The combined action of pressure and temperature on the dissolution of the GaN feedstock is depicted in Fig. 6.5. The role of the pressure value is not completely clear. A certain pressure above 2000 bar is obviously necessary to enable the formation or

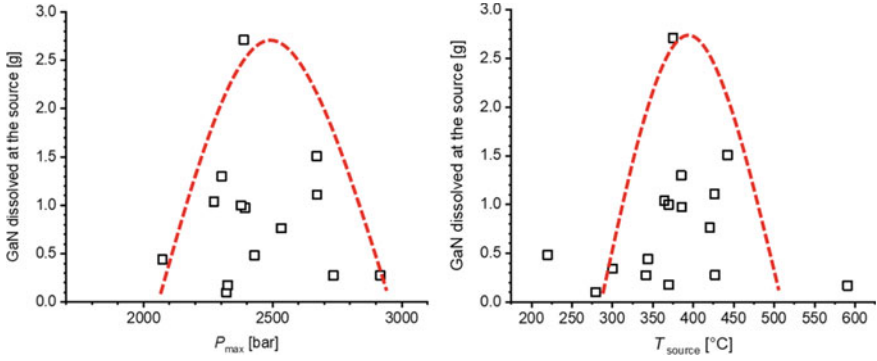


Fig. 6.4 Mass dissolution GaN at the source zone as a function of temperature at the source and pressure. The dashed lines are meant as eye guide and do not represent the fit line of a physical model

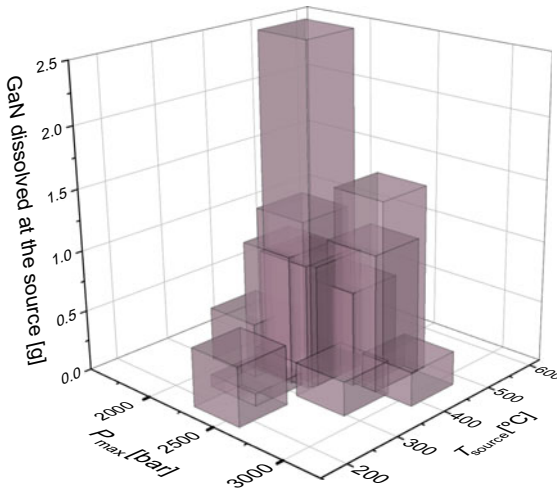


Fig. 6.5 Mass dissolution of the GaN feedstock at the place of the source in the upper part of the autoclave as a function of P and T . The plot contains all data observed, the initial concentration of mineralizer is neglected for the moment

stabilization of the complex, which dissolves the feedstock material, but the optimum condition may be a narrow space in p and T .

Figure 6.6 makes this minimum pressure threshold obvious. The graph shows the maximum measured thickness of the GaN layer which crystallized on the seed surface, plotted against the time that the system was held above 2000 bar. There is clearly a continuous increase of the deposited layer thickness with the run time above 2000 bar, which means that a stable transport and supersaturation was established and continuous growth could occur.

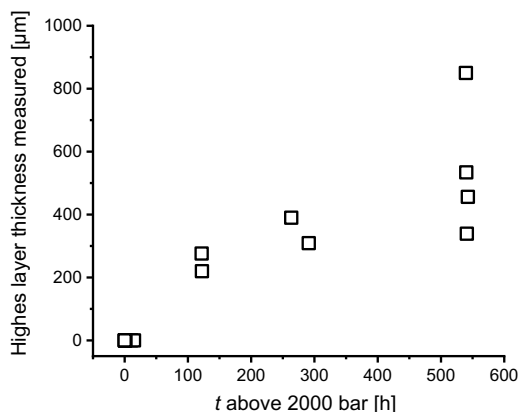


Fig. 6.6 Deposited layer thickness in relation to the process time above 2000 bar

The thickest deposited layer usually occurs on the *c*-face of the seed, which hangs on a wire in the crystallization zone at the bottom of the autoclave. Of course there is also deposition and development of crystal facets at other sides of the seed, but the amount is small compared to the *c*-face growth and hard to measure correctly, so it was neglected for the graph. In turn the question remains if all the GaN material which was dissolved at the source zone could be transported to the bottom of the autoclave and crystallized. For this contemplation we use again the data from the growth runs with a significant run time above 2000 bar and correlate the amount of grown material with the mass dissolution of GaN at the source. This includes some error as the deposition is taken as a one dimensional value and the dissolution involves the whole surface area. However, as the dissolution can be seen as the inverse growth the same argument is valid as said before. The dissolution on the side faces will be small compared to that on the *c*-face. The following graph depicts the relation between the mass dissolution at the source and the deposited material on the seed (Fig. 6.7). The relation can be taken linear for the first, which proves that at least the majority of the material dissolved at the source is transported to the crystallization zone. The fact that there is not a perfect correlation with a slope of one may result from the assumptions and inaccuracies involved in this view, including the possibility that material was deposited elsewhere in the autoclave and the fact that a solution must saturate before deposition can start. Obviously, there is anyway quite a larger number of points where a significant dissolution of material was observed but no deposition of GaN on the seeds was found. This could be even a negative value of deposition, which means that the seed was rather dissolved. The kinetic of the formation of the teraamidogallate complex is not much known under this conditions and the potassium complex is not well described in literature. Niewa et al. report the formation of complexes with Cs and other anions at much lower temperatures e. g. 350 °C [38]. Pure $K[Ga(NH_2)_4]$ as a hypothetical intermediate should be a solid compound or a liquid which is unknown with this composition so

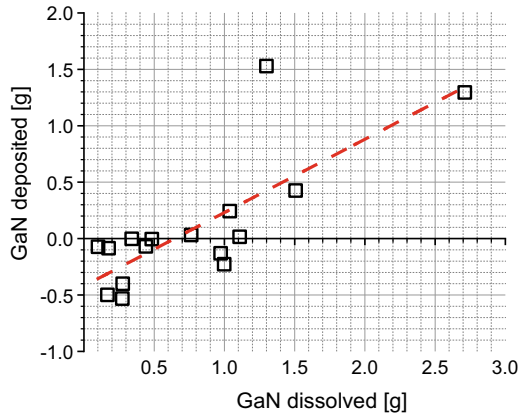
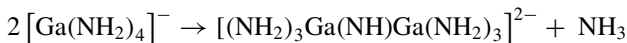


Fig. 6.7 Relation between the deposited GaN on the seed surface and the amount of mass dissolution of the GaN feedstock

far. However, the $[\text{Ga}(\text{NH}_2)_4]^-$ ion should be present in dilute form even at lower temperatures as was derived from solution NMR experiments [38]. This ion can be transported as an intermediate and dissolve the feedstock. The solution at the bottom of the autoclave may initially not be saturated and no deposition would take place. A saturation or supersaturating could be created if a more condensed species would be formed, which may happen through the action of the pressure and could explain why a minimum overpressure of at least 2000 bar would be required to create deposition at all. On the other hand the action of the pressure is not completely clear here, as from an equilibrium point of view, the pressure might not be necessary to condensate the isolated species if the concentrations are just high enough. Moreover, any solid intermediate could be eventually molten at the experimental temperatures involved. This could mean that the respective potassium-complex is formed by prominently dissolving feedstock and seeds because a supersaturation situation at the seeds cannot be created. This would be the case if either transport of that complex could not be established or concentration was even all over the autoclave. If, on the other hand a melt or liquid phase of the intermediate compound is formed as the temperature rises, it would likely take up different amounts of ammonia in relation to a given p and T condition. It can be imagined that a condensation reaction and formation of an imide compound takes place, involving various amounts of ammonia, gallium and amide ions, which would explain the involvement of an activation volume for the condensation reaction and would require a pressure activation of that process (p_{\min}):



What is really going on in the closed autoclave will still remain to be debated at the point in time, as the pressure dependence of the formation and the kinetic of the formation reaction of the potassium tetraamidogallate complex and related compounds is

unknown and was not investigated so far. Moreover, the findings described above may imply at least a two stage process which was not preconceived up to now. Otherwise this could explain why in some experiments the dissolved amount of GaN feedstock can be high even though no deposition took place.

The mass dissolution of GaN observed at the source zone could be interpreted as the dissolution of GaN taking place as a result of the formation reaction of the complex. Thus, the amount of dissolved feedstock or the dissolution rate would be mirroring the formation kinetic of the complex respectively a reaction rate of the KNH_2 and NH_3 with GaN to form the complex. This depends strongly on the total concentration of the mineralizer added to the system and probably whether it's added in form of the amide or azide. The later would, from the view of a crystal grower, mainly influence the distribution of mineralizer in the autoclave. The place and the way it is supplied to the autoclave plays a role. From experiments with sodium as a mineralizer we suspected that in case of the amide as the form of the mineralizer it was difficult to obtain a good enough dissolution of the feedstock. So the experiments with the amide were unsuccessful to a large extend. It can however not be ruled out that the amount of mineralizer was eventually too small. So far it was not possible to perform repeatable and reliable enough experiments to clarify such dependencies as the distribution of the mineralizer inside the autoclave is hard to be controlled systematically. The important difference is, that the azide compared to the amide will decompose spontaneously associated with a very short pressure peak event. This "explosion event" likely distributes the mineralizer everywhere in the autoclave including the zone of crystal growth where the seeds are located. In turn, this means that the complex can form readily everywhere in the autoclave where the Ga is available and thus dissolves the GaN at any place whether feedstock or seeds. A steady growth condition with a stable established heat and mass transport due to convection and solutal buoyancy can start only after that.

6.3.3 Presence of a Liquid Phase in Ammonobasic Crystal Growth of GaN

The out sticking difference of the experiments #2 and #3 in the above diagram 6.3 is the fact that the amount of GaN crystallized on the lowest positioned seed at the bottom of the autoclave was the highest compared to any other experiment.

In case of the KN_3 mineralizer experiments, three seeds were placed in the bottom zone of the autoclave during the growth runs. Below there is only the mineralizer as a powder. When the experiment is heated up under pressure, a sudden pressure peak occurred, which we attribute to the spontaneous decomposition of the KN_3 , whereby we suspect that the mineralizer does not remain at its original position but distributes widely in the autoclave, for a while at least. After the system reaches above the minimum pressure and temperature threshold values the formation of the complex starts everywhere in the autoclave and the GaN at the source zone will

be dissolved and transported to the growth zone, as described by the numerical models developed during the study. However, we expected that the growth of the GaN occurs differently on the 3 seeds as they are placed along the vertical axis of the autoclave which is the direction of the temperature gradient. The temperature gradient established between the source and the growth zone was about 3 K/cm, which would mean that the maximal temperature difference between the uppermost and lowest seed position would be roughly 10 K. From the findings described before in this chapter we now would conclude that this is very likely too small to see a difference between the growth on the three seeds. Anyway, the uppermost seed and the lowest could develop different due to the convection field and the related transport of the complex. The mixing at the lowest possible seed position could be expected to be most difficult and the lowest seed will have the lowest deposition rate of GaN. In fact to the majority we found a more or less comparable amount of GaN which was grown on all three seeds positioned in the autoclave. However, we found a big difference in the amount of deposited material in the case of the experiments with the accidental pressure drop. There the lowest seed had a twice as high deposited layer of GaN compared to the upper seeds, which was unexpected.

When we opened the autoclave and deglazed the residuals with water and alcohol we found a second oily liquid phase at the bottom of the glass which we used for collecting the residuals. Figure 6.8 shows a picture of the liquid captured after the opening of the autoclave.

The chemical analysis showed that a high concentration of Ga is contained in that brownish to light yellow liquid phase after reaction with the water/alcohol mixture. Liquid complexes with K, Rb and Cs were earlier described in absence of water as amido-imidogallates [37, 38]. To the best of our knowledge in none of the publications concerning the basic ammonothermal growth there was ever a description about the existence of a liquid phase as a possible liquid amidogallate complex and its involvement or possible role in the crystal growth process. However, this could help to explain the much higher growth rates for the lower placed seed, if one imagines

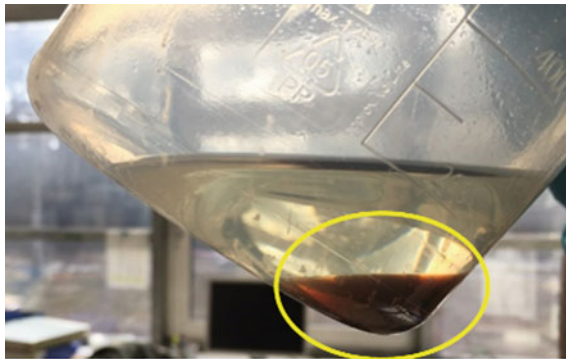


Fig. 6.8 Example of the “oily” liquid phase captured after the opening of the autoclave and washing with water and alcohol. The brownish liquid contains a high concentration of Ga

it was emerged in a Ga containing liquid during the process. In the case of a sharp pressure gradient due to depressurization, either intentionally or unintentionally (as a result of leakage), this liquid could decompose and release the Ga and forms GaN on the surface of the seeds with a high growth rate, as supersaturation can be expected to be very high in such situation. From the observations described before, it seems that the pressure is essential to stabilize the complex at higher temperatures. If a seed is immersed in the liquid phase, which forms after the heat up and pressure rise of the system to the wanted experimental conditions, a pressure gradient or pressure release will cause a fast thermal decomposition of the complex. So if a controlled thermal decomposition would be established the GaN would grow from a liquid/solution rather than from the supercritical condition, by classically reducing the solvent.

This conclusion in fact opens a wide range of options which could be tried out. One of which would be the growth from such a gallate-complex liquid without the necessity of technically harsh ammonothermal conditions. Moreover, this finding probably is also helpful to explain why the growth rates reported in literature are widely varying. The liquid phase may have been present or not or as small portion only, depending e.g. on the absolute amount of mineralizer or the positioning of the seed, but was anyway never taken into account. The picture of the chemical model and the species transport will also change accordingly. However the presence of the liquid during the process is suspected to depend also on parameters like e.g. the concentration of the mineralizer, the positioning, the pressure and temperature conditions as described before in this chapter. It would be important to clarify the existence field of potential liquid complexes experimentally and explicitly generate them in the crystal growth experiments. Based on our findings and as a hypothesis we propose exemplarily a new model of the ammonobasic crystal growth process, which will be described in the next paragraph.

6.3.4 Two Models of Ammonobasic Crystal Growth of GaN Involving a Liquid Phase

The following considerations made from a theoretical point of view, may show that the existence of a Ga-containing liquid could modify the process design and process flow of the crystal growth process fundamentally. We could envision at least two different scenarios involving the above described findings and the usage of the mineralizer either in the form of (A) the amide or (B) the azide.

In either case the GaN source material, together with the mineralizer, would form the amidogallate complex, which is necessary in order to carry the Ga. The basic difference would be that the azide will decompose spontaneously during the heating up of the autoclave, whereas the amide will either solve in the ammonia or melt and form a liquid, which localizes itself at the bottom of the autoclave if no counter measure is taken.

If one imagines an amide melt as a molten bath at the bottom of the autoclave the following processes can be considered: the amide dissolves in the supercritical ammonia until the solubility limit is reached. The same applies for the ammonia which can solve in the amide liquid. The formation of the amidogallate complex is possible where the amide anions will get into contact with the gallium. So, if the mineralizer is in form of a melt at the bottom of the set-up and the GaN source is at the top in the colder temperature zone, the amide has to reach to the top and solve the Ga from the GaN source material. However, the amount of amide created and transported to the top zone can be limited by the interface reaction between the melt and the ammonia and if the solubility limit is reached nothing will dissolve anymore. The transported amide will solve the GaN from the source and form the amidogallate complex. As the complex (as a species) is heavy compared to the other species around and in conjunction with the natural convection, the result will be the transportation and mixing of the system and the amidogallate complex can reach the GaN seeds placed at the bottom of the set-up. It is hard to imagine that the solution can be strongly supersaturated with this case and growth rates will be low. At the same time, if the amount of melt at the bottom of the autoclave is large enough, the seeds could have been accidentally immersed in the liquid. This would result first in rather a dissolution of the seeds exposed to the melt, unless the amide melt is saturated with Ga, or the complex had formed at the interface to the ammonia. However, not much more GaN will grow as was dissolved before. Further growth by additional complex transported from the top part will likely be diffusion limited and limited by the interface kinetic at the melt-ammonia interface. This was visible from some of our experiments where we would have expected the growth of GaN with respect to the p and T conditions, but in fact found a negative growth rate. Moreover, the dissolution of GaN seeds at the bottom was much higher than the amount of GaN dissolved from the source GaN blocks. This could be explained with the existence of a melt and the processes described above. If taken into account that the amide is thought to have retrograde solubility in ammonia this scenario could be even worse. The same would apply if the amount of mineralizer would be too small, such that a melt residue cannot be formed. Proper supersaturation can then hardly be expected.

If one discusses the rate limiting steps, the concentration of the complex could be determined by the kinetic of the formation reaction of the complex at the surface of the amide melt or the decomposition pressure of the amide under temperature and pressure, which is unknown to our knowledge. In a case where the mineralizer would not be applied in excess, such that an amide liquid can be imagined, the picture of low growth rates remains the same. This would even not change much, if the mineralizer would be put in the top part around the GaN source at the beginning instead of beneath the seeds. If the amide melt would be stable under the applied pressure it could drop down from the source basket to form the melt bath or if put in a closed container the melt would stay there and the same surface reactions would be rate limiting, adding the step that the complex would have to diffuse out of the container. In this way the picture probably does more represent the actual vision of the ammonbasic process including the reported growth rates, which are typically low. To the above considerations one could expect that a huge amount of back etching from the seed

surface should be involved in the case (A). This is in principle to the majority of aspects positive, but must be compensated before a positive growth rate is achieved, which is unpleasant in front of low growth rates. Unfortunately, back etching was not studied fundamentally for the ammonothermal crystal growth and no systematic publications exist. In fact, this also adds uncertainties to observed growth rates. It is hard to discuss this detailed to its full extend, as the data in the literature is very diverse, the governing parameters are many and the materials data like solubility of different amides in NH_3 under pressure and temperature is not known. In the following Fig. 6.9 we sketched the proposed case (A) with the usage of e.g. K-amide as mineralizer, placed at the bottom of the autoclave. The amount of amide in powder form is not pictured in true scale to the amount of liquid expected, this was chosen for better visualization. It is more likely, that the amount of powder would be more than the height of the meniscus of the corresponding melt. The Ga entering the amide liquid is drawn as a halo around the seed crystal pictogram, indicating the existence of a concentration gradient of Ga. In fact such a gradient around a dissolving GaN crystal was observed in an in situ x-ray imaging experiment by Schimmel et al. [39] (and see also Chap. 10 of this book) and would contribute another little confirmation of the here proposed semi empirical model. In the figure the amidogallate complex is given as $[\text{Ga}(\text{NH}_2)_4]^-$.

In contrast to the case (A) the usage of the azide, case (B), will lead early in the process to an explosive decomposition of the mineralizer with fast distribution all over the volume of the reaction vessel. The amide ions will be formed everywhere

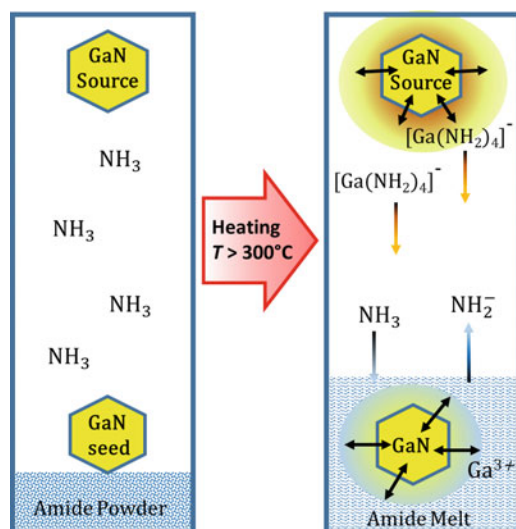


Fig. 6.9 Schematic drawing of the case (A) where the mineralizer is put at the bottom of the autoclave in form of an amide powder. In the second step the amide forms a melt situated at the bottom of the autoclave which can surround the seeds. The situation of a seed possibly placed above the melt surface is not drawn here. Other details are given in the text

in the autoclave and find access to the GaN source immediately. At that point in the process no liquid phase is involved so far, but the amidogallate complex can form readily. The formation reaction would be limited by the available interface area to a Ga containing source compound, which is the surface of the GaN source blocks. If the process condition with respect to p and T are such that the experiment falls into the stability field of the complex, which may exist in form of a liquid as discussed before, that can segregate to the bottom of the autoclave and could or could not immerse the seeds. The fundamental difference would be, that in the case (A) the liquid phase would be an amide and in case (B) the liquid phase would be the amidogallate complex. The amidogallate is now already saturated with Ga such that the GaN seed crystals see no driving force to dissolve. Consequently, back etching should not be a big issue here. As the bottom is the hotter zone, the complex can thermally dissociate and release the Ga. As the GaN seed surfaces offers the energetic sink, a GaN layer will grow with probably no or only few back etching that could have appeared in case (A) before. The free amide ions can be transported back to the source and bring about additional Ga and the complex compound forms again. The latter case can probably exhibit higher growth rates compared to case (A) if performed under optimized conditions or in a different way as will be discussed later. The case (B) is sketched in the following Fig. 6.10.

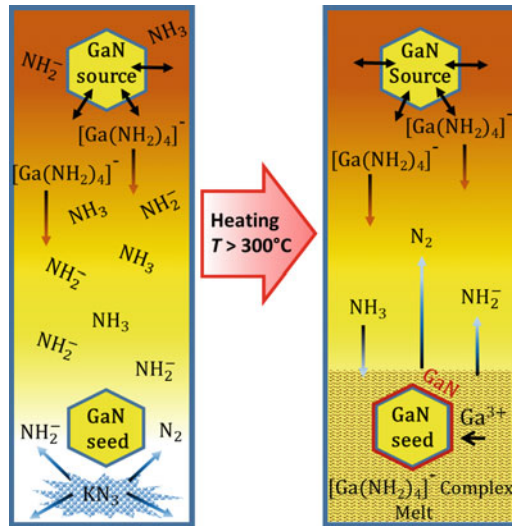


Fig. 6.10 Schematic drawing of the case (B) where the mineralizer is put at the bottom of the autoclave in form of an azide powder. After explosive azide decomposition the amidogallate complex will form readily everywhere in the volume. In the second step a melt formed by the amidogallate may exist at the bottom of the autoclave which could also surround the seeds. This melt is already saturated with Ga and GaN can grow onto the surface of the seeds easily. The condition of a seed possibly placed above the melt surface is not drawn here. Other details are given in the text

Table 6.1 Summary of the major differences and consequences between case (A) and case (B) or the application of an amide or azide mineralizer respectively

	Case A	Case B
Mineralizer-type	Amide	Azide
Limiting step for the formation of the complex	Solubility of amide mineralizer in supercritical ammonia	Surface area of the GaN source blocks
	Solution kinetic via the melt surface	Kinetic of the formation reaction
	Formation reaction at the surface of the melt	Thermal decomposition of the complex melt
Expected growth rate	Low	High
Expected supersaturation	Low	High
Expected backetching	High	Low
Dissolution rate at source	Low	High

Also in the case (B) the mineralizer could be as well placed around the GaN source blocks, which may change the amount of GaN readily solved. However, it would not change the principal picture discussed with case (B).

In the following Table 6.1 the major differences between the two cases are compiled, showing what consequences would be expectable due to the choice of an alkali amide or azide as a mineralizer.

6.3.5 *New Perspective for the Growth of GaN from Amidogallate Liquids*

In fact considering all the findings discussed here, the consequence for the crystal growth may be various and potentially groundbreaking, including a complete novel perspective for the design of the ammonothermal growth in a basic regime. Even though the picture drawn here contains speculative aspects, which need of cause additional prove, there is enough experimental basis also in conjunction with parallel findings from the other researchers reporting their studies in this book, to make this a valid hypotheses. The most jolting finding is unambiguously the existence of an amidogallate complex in a liquid form during the growth process, which offers a different perspective and options. It promotes a suggestion for a complete new growth process based on the thermal decomposition of the liquid amidogallate. The fundament is, that this liquid is already saturated with nitrogen and gallium ions with respect to the wanted compound (GaN) that should be crystallized. Hertrampf et al. [38] discussed the condensation reaction of the dissolved intermediates towards GaN and the action of access ammonia which obviously stabilizes the complex intermediate ions. This condensation would function even at temperatures as low as

room temperature. This implies also, that the assumption made in the model of case (B) as discussed above, that the GaN had crystallized from the amide complex liquid is very valid. Principally, the alkali metal amidogallate complexes, at least K-, Rb-, and Cs-amidogallates, could be synthesized individually as a liquids or amorphous solids. All show a significant vapour pressure and release ammonia if not kept sealed or under respective gas atmosphere, which means that the compounds can be stable in form of a liquid if kept under overpressure. As the vapour pressure likely increases if the compound is heated, the necessary required overpressure may rise to higher values. In turn this implies that the amidogallate complex could exist in liquid form under a high pressure like applied in the ammonothermal crystal growth regime and suggested by our before described experiments.

In consequence this would offer the opportunity to directly load the complex as solid or liquid into the autoclave and place the GaN seeds directly inside the liquid. The reaction vessel should then be filled with liquid ammonia to some excess. The liquid can be considered as a presaturated solvent. As for the crystallization the system has to be heated, the vessel will become pressurized. The fundamental principle of crystallizing the GaN out of the liquid, due to subsequent decomposition or reduction of the solvent would be a very classical way of crystal growth. The technique of flux evaporation has various advantage including the possibility of isothermal growth, provided the fact that the vapor pressure of the flux is high enough, which is indeed the case. Usually the evaporation is established by thermal decomposition of the solvent. Under the given circumstances with the amidogallate complexes, the decomposition of the flux could also be established by controlled lowering of the system pressure at constant temperature.

From the experimental observations made in our study we can conclude that lowering the pressure at constant temperature would effectively decompose the complex and release the GaN. However, controlling crystal growth by slow depressurization is quite difficult. So as an alternative the thermal decomposition at constant pressure can be taken as another option. Temperature control can be established quite easily and is uncritical even up to higher temperatures if the total applied pressure is low or medium high. This means by direct usage of the amide complex-liquid under excess ammonia and subsequent slow thermal decomposition, a GaN crystal growth could be established. The striking advantage could be, that such a process may need an overpressure and some temperature but by no means such harsh conditions, like the actual used ammonothermal temperature and pressure values. In turn for such a process one would not have to deal with retrograde solubility and would be undoubtedly easier to control and observe. Prerequisite would be to finally study the stability field of amidogallat complexes and related melts in a p, T diagram in more detail.

Figure 6.11 shows the picture of a crystal grown on a rounded seed at the very bottom of the autoclave likely surrounded by the K-amidogallate liquid. The seed was a piece of GaN grinded round as a cylinder and no crystal direction was offered prominently for further growth. We called this the “kinetic seeds” This is a classical experiment. The crystal can develop freely the respective equilibrium shape for the given condition.

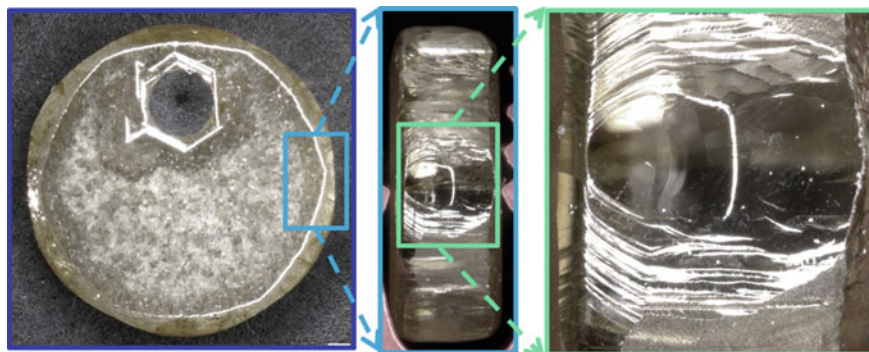


Fig. 6.11 Picture of the growth on the surface of a so called “kinetic seed” which was a piece of round grinded, cylinder shaped GaN

The hole in the seed was made for hanging the seed in a wire. It is visible that the pure cylinder shape changed and developed a natural faceted hexagonal crystal habit. The faces are mirror like flat and show stepped edges. It seems that the supersaturation was almost evenly distributed around the seed, thus growth could occur in any direction and the growth rate seems to be equal in any direction of the hexagonal prism. The basal plane directions (along the c -axis) grew fastest, at both c -directions evenly. As a conclusion the seeds must have been within a condition of metastable supersaturation, the so called Ostwald Miers regime. This observation is consequent if imagined that the seed came to lay inside the amidogallate liquid at the bottom of the autoclave and grew from the liquid.

6.4 Conclusions

The study of the basic ammonothermal regime reported here resulted in a better understanding of the ongoing processes in the autoclave. The first chemical model proposed and the later observation of a liquid phase after the opening of the autoclave in conjunction with the findings described by other colleagues here in this book not only lead to explanations for the experiments performed and discussed in this chapter, but also to a new hypothesis about the understanding of the basic ammonothermal crystal growth process in a different way. The dependencies of parameters are however manifold e.g. the type and amount of mineralizer, the place where it's being put in the autoclave, the places of the seeds, p and T , etc., which could help to explain e.g. the different growth rates or solubilities reported in literature. More studies concentrating on the intermediate species are necessary in order to achieve a full picture of the processes going on during basic ammonothermal crystal growth.

Even though some of the discussion contains speculative aspects the hypothesis made is justified.

This in turn made it possible to suggest a novel solvent evaporation growth process based on an alkali metal amidogallate liquid where crystal seed could be dipped into the amidogallate melt and the GaN could grow by thermal decomposition of the complex. Such a process would be a novelty and was never demonstrated for nitride crystal growth although different solution growth methods were tried. However, it is subject to further work to prove that suggestion and try it out experimentally.

References

1. G. Meneghesso, M. Meneghini, E. Zanoni, Gallium Nitride-enabled High Frequency and High Efficiency Power Conversion (Springer International Publishing, 2018)
2. H. Amano et al., The 2018 GaN power electronics roadmap, 1. Manufacturing challenges of GaN-on-Si HEMTs in a 200 mm CMOS fab. *J. Phys. D: Appl. Phys.* **51**, 163001 (2018)
3. D. Ehretraut, N. Hoshino, Y. Kagamitani, A. Yoshikawa, T. Fukuda, H. Itoh, S. Kawabata, Temperature effect of ammonium halogenides as mineralizers on the phase stability of gallium nitride synthesized under ammonothermal conditions. *J. Mater. Chem.* **17**, 886–893 (2007)
4. D. Ehretraut, M. Bockowski, E. Meissner, Technology of Gallium Nitride Crystal Growth (Springer, Berlin, New York, 2010)
5. A. Tenten, Amide und Nitride von Nickel, Palladium und Platin sowie von Aluminium, Gallium und Indium. Doctoral Dissertation, Universität Dortmund (1991)
6. R. Guarino, J. Rouxel, L'amidogallate de potassium $\text{KGa}(\text{NH}_2)_4$ et l'imidogallate $\text{KGa}(\text{NH})_2$. L'obtention de l'amidure de gallium $\text{Ga}(\text{NH}_2)_3$. *Bull. Soc. Chim. Fr.* **7**, 2284–2287 (1969)
7. S. Zhang, Intermediates During the Formation of GaN under Ammonothermal Conditions. Doctoral Dissertation, Universität Stuttgart (2014)
8. J. Erlekampf, J. Seebeck, P. Savva, E. Meissner, J. Friedrich, N.S. Alt, E. Schlücker, L. Frey, Numerical time-dependent 3D simulation of flow pattern and heat distribution in an ammonothermal system with various baffle shapes. *J. Crystal Growth* **403**, 96–104 (2014)
9. J. Seebeck, P. Savva, J. Erlekampf, E. Meissner, J. Friedrich, L. Frey, Species transport by natural convection of supercritical ammonia, in Turbulence, Heat and Mass Transfer, 8, Begell House, Inc. (2015)
10. R. Dwilinski, R. Doradziński et al., Bulk ammonothermal GaN. *J. Crystal Growth* **311**, 3015–3018 (2009)
11. R. Kudrawiec et al., Nonpolar GaN substrates grown by ammonothermal method. *Appl. Phys. Lett.* **93**, 061910 (2008)
12. T. Hashimoto, M. Saito et al., Seeded growth of GaN by the basic ammonothermal method. *J. Cryst. Growth* **305**, 311–316 (2007)
13. M. Saito, D.S. Kamber, Plane dependent growth of GaN in supercritical basic ammonia. *Appl. Phys. Express* **1**, 121103 (2008)
14. B. Wang, M.J. Callahan, K.D. Rakes, L.O. Bouthillette, S.-Q. Wang, D.F. Bliss, J.W. Kolis, Ammonothermal growth of GaN crystals in alkaline solutions. *J. Cryst. Growth* **287**, 376–380 (2006)
15. T. Hashimoto, F. Wu, J.S. Speck, S. Nakamura, Growth of bulk GaN crystals by the basic ammonothermal method. *Jpn. J. Appl. Phys.* **2**, 889–891 (2007)
16. D. Bliss, B. Wang, M. Suscavage et al., Ammonothermal GaN: morphology and properties. *J. Cryst. Growth* **312**, 1069–1073 (2010)
17. D. Tomida, Y. Kagamitani, Q. Bao, K. Hazu, H. Sawayama, S.F. Chichibu, C. Yokoyama, T. Fukuda, T. Ishiguro, Enhanced growth rate for ammonothermal gallium nitride crystal growth using ammonium iodide mineralizer. *J. Cryst. Growth* **353**, 59–62 (2012)

18. R. Kucharski, M. Zajac, R. Doradziński, M. Rudziński, R. Kudrawiec, R. Dwiliński, Non-polar and semi-polar ammonothermal GaN substrates. *Semicond. Sci. Technol.* **27**, 024007 (2012)
19. G.G.C. Arizaga, G.S. Herrera, A.M. Fischer, O.E.C. López, Influence of reaction conditions on the growth of GaN rods in an ammono-CVD reactor. *J. Cryst. Growth* **319**, 19–24 (2011)
20. T. Li, G. Ren et al., Growth behavior of ammonothermal GaN crystals grown on non-polar and semi-polar HVPE GaN seeds. *Cryst. Eng. Comm.* **21**, 4874–4879 (2019)
21. P. Hartman, W.G. Perdock, On the relations between structure and morphology of crystals. I, *Acta Crystallogr.* **8**, 49–52 (1955)
22. R.F.P. Grimbergen, H. Meekes, P. Bennema, C.S. Strom, L.J.P. Vogels, On the prediction of crystal morphology. I. The Hartman-Perdok theory revisited. *Acta Crystallogr. A* **54**, 491–500 (1998)
23. P. Bennema, H. Meekes, S.X.M. Boerrigter, H.M. Cuppen, M.A. Deij, J. van Eupen, P. Verwer, E. Vlieg, Crystal growth and morphology: new developments in an integrated Hartman–Perdok connected net roughening transition theory, supported by computer simulations. *Cryst. Growth & Design* **4**, 905–913 (2004)
24. L.N. Rashkovich, G.T. Moldazhanova, Growth kinetics and bipyramid-face morphology of KDP crystals, in *Growth of Crystals*, vol. 20, ed. by E.I. Givargizov, A.M. Melnikova (Springer, Boston, MA, 1996)
25. M. Rak, N.N. Eremin, T.A. Eremina et al., On the mechanism of impurity influence on growth kinetics and surface morphology of KDP crystals-I. *J. Cryst. Growth* **273**, 577–585 (2005)
26. T.A. Eremina, V.A. Kuznetsov, N.N. Eremin, T.M. Okhrimenko, N.G. Furmanova, E.P. Efremova, M. Rak, On the mechanism of impurity influence on growth kinetics and surface morphology of KDP crystals-II. *J. Cryst. Growth* **273**, 586–593 (2005)
27. F. Abbona, D. Aquilano, Morphology of crystals grown from solutions, in *Springer Handbook of Crystal Growth* (Springer, Berlin, Heidelberg, 2010). ISBN 978-3-540-74182-4
28. S. Pimpitkar, S. Kawabata, J.S. Speck, S. Nakamura, Improved growth rates and purity of basic ammonothermal GaN. *J. Cryst. Growth* **403**, 7–17 (2014)
29. D. Ehrentraut, R. T. Pakalapati, D. S. Kamber, W. Jiang, D. W. Pocius, B. C. Downey, M. McLaurin, M. P. D’Evelyn, High quality, low cost ammonothermal bulk GaN substrates. *Jpn. J. Appl. Phys.* **52**, 08JA01 (2013)
30. N.S.A. Alt, E. Meissner, E. Schluecker, In situ monitoring technologies for ammonothermal reactors. *Phys. Status Solidi C* **9**, 436–439 (2012)
31. Q.-S. Chen, V. Prasad, W.R. Hu, Modeling of ammonothermal growth of nitrides. *J. Cryst. Growth* **258**, 181–187 (2003)
32. Y. Masuda, A. Suzuki, T. Ishiguro, Y. Chiaki, Numerical simulation of heat and fluid flow in ammonothermal GaN bulk crystal growth process. *Jpn. J. Appl. Phys.* **52**, 08JA05 (2013)
33. Y.-N. Jiang, Q.-S. Chen, V. Prasad, Numerical simulation of ammonothermal growth processes of GaN crystals. *J. Cryst. Growth* **318**, 411–414 (2011)
34. S. Pendurtia, Q.-S. Chen, V. Prasad, Modeling ammonothermal growth of GaN single crystals: the role of transport. *J. Cryst. Growth* **296**, 150–158 (2006)
35. S. Zhang, N.S.A. Alt, E. Schlücker, R. Niewa, Novel alkali metal amidogallates as intermediates in ammonothermal GaN crystal growth. *J. Cryst. Growth* **403**, 22–28 (2014)
36. P. Molinie, R. Brec, J. Rouxel, P. Herpin, Structures des amidoaluminates alcalins MAI(NH₂)₄ (M = Na, K, Cs). Structure de l’ amidogallate de sodium NaGa(NH₂)₄. *Acta Crystallogr. B* **29**, 925–934 (1973)
37. B. Wang, M.J. Callahan, Transport growth of GaN crystals by the ammonothermal technique using various nutrients. *J. Cryst. Growth* **291**, 455–460 (2006)
38. J. Hertrampf, E. Schlücker, D. Gudat, R. Niewa, Dissolved intermediates in ammonothermal crystal growth: stepwise condensation of [Ga(NH₂)₄][−] toward GaN. *Cryst. Growth Des.* **17**, 4855–4863 (2017)
39. S. Schimmel, M. Lindner, T.G. Steigerwald, B. Hertweck, T.M.M. Richter, U. Künecke, N.S.A. Alt, R. Niewa, E. Schlücker, P. Wellmann, Determination of GaN solubility in supercritical ammonia with NH₄F and NH₄Cl mineralizer by in situ x-ray imaging of crystal dissolution. *J. Cryst. Growth* **418**, 64–69 (2015)